

# A model of the vertical apparent mass and the fore-and-aft cross-axis apparent mass of the human body during vertical whole-body vibration

Naser Nawayseh<sup>a,\*</sup>, Michael J. Griffin<sup>b</sup>

<sup>a</sup>*Mechanical Engineering Department, College of Engineering, Dhofar University, PO Box 2509, Postal Code 211 Salalah, Sultanate of Oman*

<sup>b</sup>*Human Factors Research Unit, Institute of Sound and Vibration Research, University of Southampton, Southampton SO17 1BJ, UK*

Received 28 June 2007; received in revised form 18 May 2008; accepted 26 May 2008

Handling Editor: A.V. Metrikine

Available online 3 July 2008

---

## Abstract

The apparent mass of the human body reflects gross movements caused by whole-body vibration and can be used to predict the influence of body dynamics on seat transmissibility. With vertical excitation, various models fit the measured vertical apparent mass of the human body, but experiments also show high fore-and-aft forces on the seat (the fore-and-aft cross-axis apparent mass) that have not influenced current models. This paper defines a model that predicts the vertical apparent mass and the fore-and-aft cross-axis apparent mass of the seated human body during vertical excitation. A three degree-of-freedom model with vertical, fore-and-aft and rotational (i.e. pitch) degrees of freedom has been developed with twelve model parameters (representing inertia, stiffness, damping, and geometry) optimised to the measured vertical apparent mass and the measured fore-and-aft cross-axis apparent mass of the body. The model provides close fits to the moduli and phases for both median data and the responses of 12 individual subjects. The optimum model parameters found by fitting to the median apparent mass of 12 subjects were similar to the medians of the same parameters found by fitting to the individual apparent masses of the same 12 subjects. The model suggests the seated human body undergoes fore-and-aft motion on a seat when exposed to vertical excitation, with the primary resonance frequency of the apparent mass arising from vertical motion of the body. According to the model, changes in the vertical, fore-and-aft, or rotational degree of freedom have an effect on the resonance in the fore-and-aft cross-axis apparent mass.

© 2008 Elsevier Ltd. All rights reserved.

---

## 1. Introduction

Experimental studies show considerable cross-axis fore-and-aft forces on a seat induced by vertical whole-body vibration [1–3]. The forces show that the seated human body moves in at least two dimensions when exposed to vertical vibration—consistent with rotational modes of the pelvis, the spine, and the upper body [1,4]. Such motions will result in both axial and shear cross-axis forces in the spine [5]. Including the cross-axis

---

\*Corresponding author.

E-mail address: [nnawayseh@yahoo.co.uk](mailto:nnawayseh@yahoo.co.uk) (N. Nawayseh).

forces in mathematical models of the responses of the human body to vibration should improve understanding of how the human body moves during vibration. It may also advance understanding of some effects of vibration on the human body.

Most biodynamic models allow the prediction of forces in the direction of excitation (e.g. Refs. [6–11] for vertical excitation and Refs. [12,13] for horizontal excitation). The structures of the various models range from one to many degrees of freedom (e.g. Refs. [8,9]). However, it has been shown that a two degree-of-freedom model can provide a highly accurate representation of the modulus and phase of the vertical apparent masses of seated subjects in the direction of excitation at frequencies less than about 20 Hz [8].

Using measurements of the transmissibility to the upper body, a few models have taken into account the cross-axis movements of the body induced by vertical excitation (e.g. Refs. [14,15]). Nawayseh [16] described a two degree-of-freedom model that represented the modulus of vertical apparent mass and fore-and-aft cross-axis apparent mass (complex ratio of fore-and-aft force measured on the seat and vertical acceleration), but only for frequencies less than 6 Hz.

This paper presents a three degree-of-freedom model that can predict the vertical apparent mass and the fore-and-aft cross-axis apparent mass during vertical excitation. A three degree-of-freedom model was investigated because a model of the vertical apparent mass alone requires at least two degrees of freedom [8]. The results of Nawayseh [16] suggest the need for a third degree-of-freedom to accommodate the fore-and-aft cross-axis apparent mass. It was hypothesised that at least a three degree-of-freedom model with rotational capability would be needed to predict both the vertical apparent mass and the fore-and-aft cross-axis apparent mass during vertical excitation. The proposed model can be used to predict the vertical and fore-and-aft forces on a seat when vibration excitation is dominantly in the vertical direction. The model could be a first step toward more complex nonlinear models of biodynamic response to multi-axial vibration where the apparent mass in one direction is dependent on the vibration in that direction and also the vibration in other directions [17–19].

## 2. Model description

The proposed model is a three degree-of-freedom model with vertical, fore-and-aft, and rotational motion (Fig. 1). The rotational degree of freedom is needed to predict the fore-and-aft force on the seat induced by vertical excitation. The translational and rotational springs and translational and rotational dampers used in the model have linear excitation-response relationships. The model obviously is not intended to represent the full complexity of motions occurring in the seated human body during vertical vibration excitation—it is developed as one of the simplest possible configurations providing a close approximation to the vertical apparent mass and cross-axis fore-and-aft apparent mass of the body.

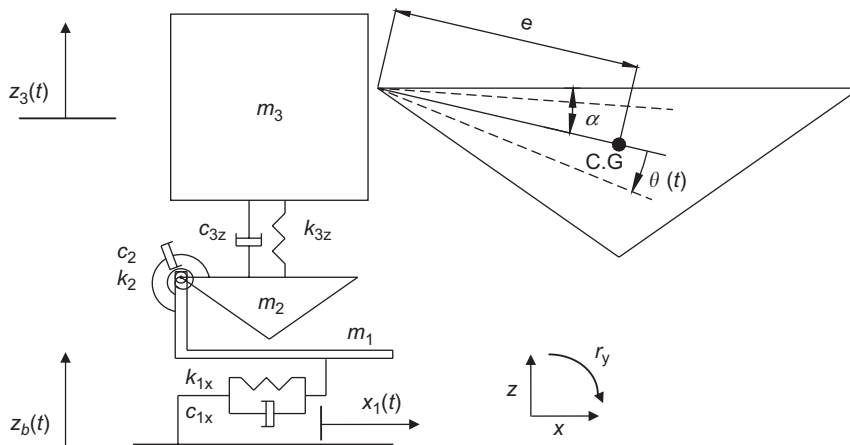


Fig. 1. Lumped parameter model for the seated human body exposed to vertical vibration.

The vertical apparent mass and fore-and-aft cross-axis apparent mass data used in this paper are those obtained experimentally [1] with 12 subjects seated with an ‘average thigh contact’ posture (upper legs horizontal and lower legs vertical) on a rigid seat with no backrest and measured with vertical excitation at a vibration magnitude of  $1.25 \text{ m s}^{-2}$  rms (the moduli and phases of the apparent masses and cross-axis apparent masses measured in Ref. [1] are reproduced in Figs. 2–6). The human body has a nonlinear response to both vertical and fore-aft excitation, so different vibration magnitudes produce a different response. The parameters obtained for the model in this paper apply to a vertical random excitation of  $1.25 \text{ m s}^{-2}$  rms and for people sitting on a rigid seat without a backrest adopting an average thigh contact posture (upper legs horizontal and lower legs vertical).

2.1. Equations of motion

The equations of motion of the model were derived using Lagrange’s equations (Eqs. (1–3)). It should be noticed that the rotational motion of mass 2 induces only vertical motion of mass 3, while the horizontal degree of freedom beneath mass 1 allows mass 1, mass 2, and mass 3 to move in the horizontal direction. For rotational motion, counter-clockwise rotation was considered positive:

$$m_3 \frac{d^2 z_3}{dt^2} + c_{3z} \left( \frac{dz_3}{dt} - \frac{dz_b}{dt} + e \cos \alpha \frac{d\theta}{dt} \right) + k_{3z}(z_3 - z_b + e\theta \cos \alpha) = 0 \tag{1}$$

$$m_1 \frac{d^2 x_1}{dt^2} + m_2 \left( \frac{d^2 x_1}{dt^2} + e \sin \alpha \frac{d^2 \theta}{dt^2} \right) + m_3 \frac{d^2 x_1}{dt^2} + c_{1x} \frac{dx_1}{dt} + k_{1x} x_1 = 0 \tag{2}$$

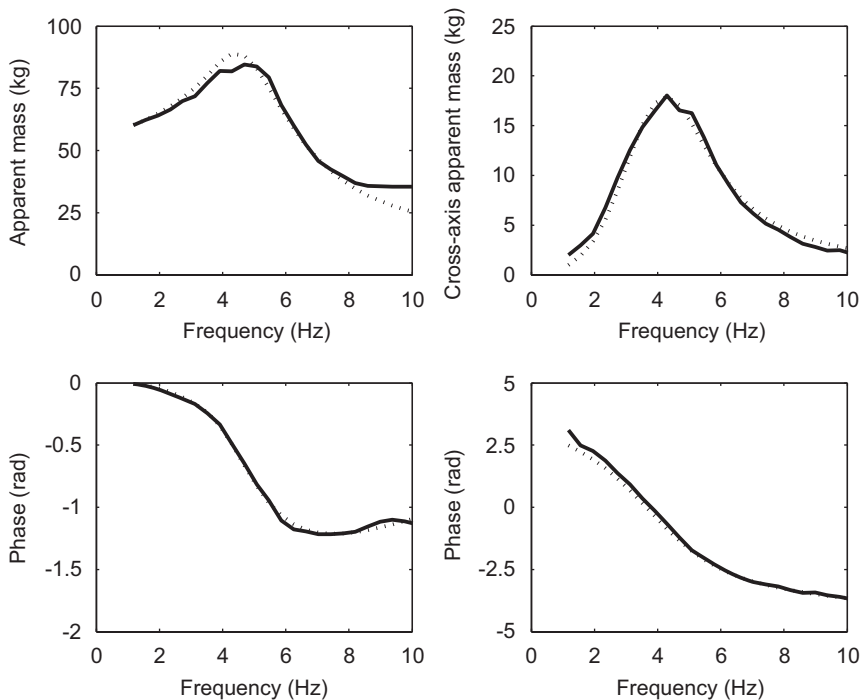


Fig. 2. Modulus and phase of the median vertical apparent mass and fore-and-aft cross-axis apparent mass of 12 subjects: —, measured; · · · · ·, predicted.

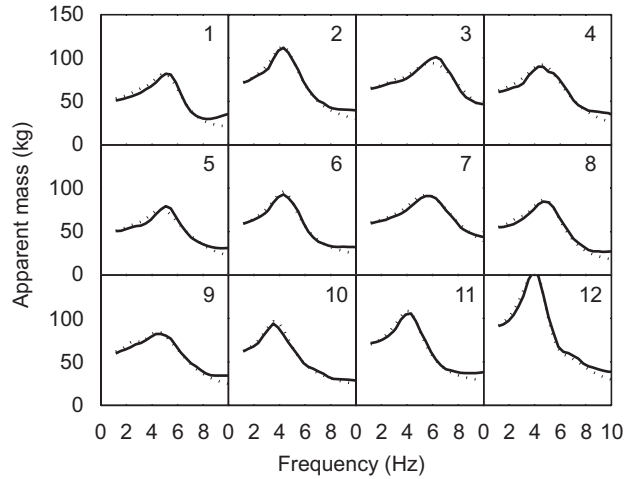


Fig. 3. Modulus of the vertical apparent masses of 12 subjects: —, measured; · · · · ·, predicted.

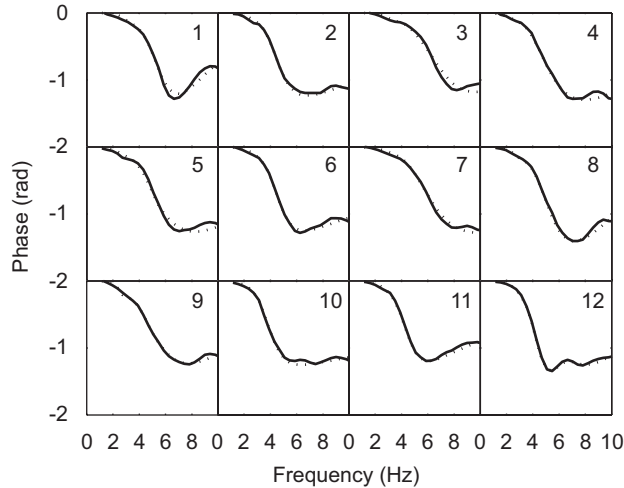


Fig. 4. Phase of the vertical apparent masses of 12 subjects: —, measured; · · · · ·, predicted.

$$\begin{aligned}
 & m_2 e \cos \alpha \frac{d^2 z_b}{dt^2} + m_2 e \sin \alpha \frac{d^2 x_1}{dt^2} + J_2 \frac{d^2 \theta}{dt^2} + c_{3z} e \cos \alpha \left( \frac{dz_3}{dt} - \frac{dz_b}{dt} + e \cos \alpha \frac{d\theta}{dt} \right) \\
 & + k_{3z} e \cos \alpha (z_3 - z_b + e \theta \cos \alpha) + c_2 \frac{d\theta}{dt} + k_2 \theta = 0
 \end{aligned} \tag{3}$$

where  $J_2 = m_2 e^2 + I_2$

The following nomenclatures will be used when referring to the parameters of the model:

- $e$  is the distance between the centre of gravity of mass 2 and the connection point
- $I_2$  is the moment of inertia of mass 2 about its centre of gravity
- $J_2$  is the moment of inertia of mass 2 about the connection point
- $k_{1x}$  and  $c_{1x}$  are the fore-and-aft stiffness and damping beneath mass 1
- $k_2$  and  $c_2$  are the rotational stiffness and damping of mass 2
- $k_{3z}$  and  $c_{3z}$  are the vertical stiffness and damping beneath mass 3
- $m_1, m_2$  and  $m_3$  are the masses of mass 1, 2 and 3, respectively
- $t$  the time

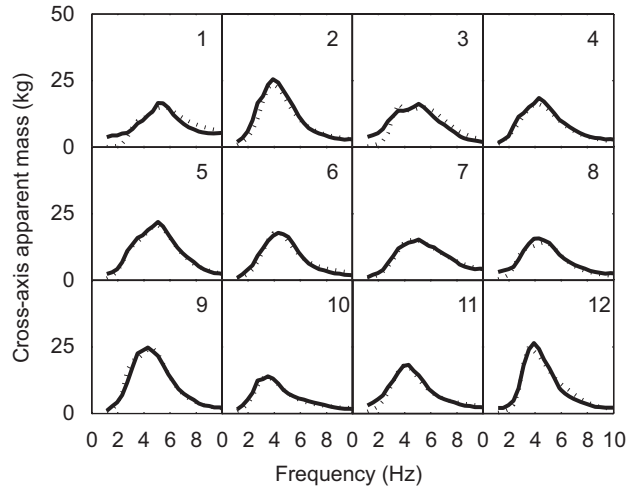


Fig. 5. Modulus of the fore-and-aft cross-axis apparent masses of 12 subjects: —, measured; ·····, predicted.

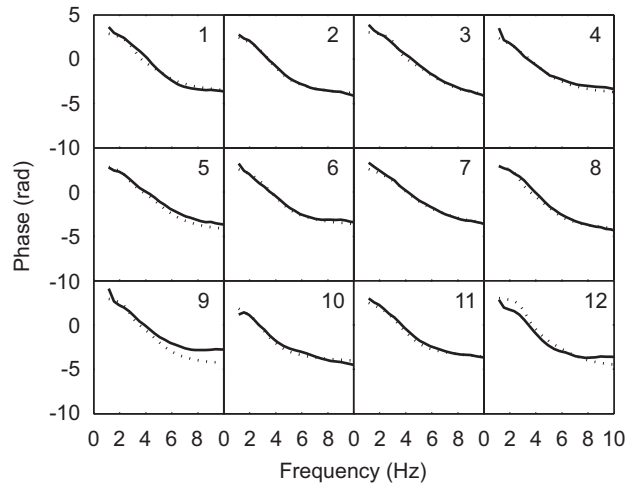


Fig. 6. Phase of the fore-and-aft cross-axis apparent masses of 12 —, measured; ·····, predicted.

$x_1$  the fore-and-aft displacement

$z_3$  the vertical displacement of mass 3

$z_b$  the vertical displacement of the base

$\alpha$  the angle that  $e$  has with the horizontal when the model is in equilibrium (see Fig. 1)

$\theta$  the rotational displacement of mass 2

The total vertical and fore-and-aft forces produced in the model are given by the following equations:

$$f_z(t) = m_1 \frac{d^2 z_b}{dt^2} + m_2 \left( \frac{d^2 z_b}{dt^2} + e \cos \alpha \frac{d^2 \theta}{dt^2} \right) + m_3 \frac{d^2 z_3}{dt^2} \tag{4}$$

$$f_x(t) = (m_1 + m_2 + m_3) \frac{d^2 x_1}{dt^2} + m_2 e \sin \alpha \frac{d^2 \theta}{dt^2} \tag{5}$$

where  $f_z(t)$ , force in the vertical direction at the interface between the body and the seat surface;  $f_x(t)$ , force in the fore-and-aft direction at the interface between the body and the seat surface; the vertical apparent mass of the model is then calculated from the complex ratio of the total force in the vertical

direction,  $f_z(t)$ , and the acceleration,  $z_b(t)$  (Eq. (6)). The fore-and-aft cross-axis apparent mass is calculated from the complex ratio of the force in the fore-and-aft direction,  $f_x(t)$  and the acceleration,  $z_b(t)$  (Eq. (7)).

$$M(\omega) = \frac{S_{a_z f_z}(\omega)}{S_{a_z a_z}(\omega)} \quad (6)$$

$$M_C(\omega) = \frac{S_{a_z f_x}(\omega)}{S_{a_z a_z}(\omega)} \quad (7)$$

where  $M(\omega)$  and  $M_C(\omega)$  are the apparent mass and the cross-axis apparent mass, respectively,  $S_{a_z f_z}(\omega)$  and  $S_{a_z f_x}(\omega)$  are the cross-spectral density between the vertical force and the vertical acceleration and the cross-spectral density between the horizontal force and vertical acceleration, respectively, and  $S_{a_z a_z}(\omega)$  is the power spectral density of the vertical acceleration.

## 2.2. Procedure

All model parameters (inertia properties, stiffness, damping coefficients, and location of the centre of gravity of mass 2) were optimised using the Nelder Meade simplex search method provided in MATLAB (version 6.1) by comparing the calculated responses of the model with the results obtained experimentally by Nawayseh and Griffin [1]. The frequency range of the optimisation was 1–10 Hz. The moduli and phases of both the vertical apparent mass and the fore-and-aft cross-axis apparent mass were used to minimise the error between the responses of the model and the measured data as

$$\text{err} = \sum_{i=1}^N (M_p - M_m)_i^2 + w_1 \sum_{i=1}^N (M_{C_p} - M_{C_m})_i^2 + w_2 \sum_{i=1}^N (\Phi_p - \Phi_m)_i^2 + w_3 \sum_{i=1}^N (\Phi_{C_p} - \Phi_{C_m})_i^2 \quad (8)$$

where  $M_p$  and  $M_{C_p}$ , predicted vertical apparent mass and fore-and-aft cross-axis apparent mass, respectively;  $M_m$  and  $M_{C_m}$ , measured vertical apparent mass and fore-and-aft cross-axis apparent mass, respectively;  $\Phi_p$  and  $\Phi_{C_p}$ , predicted phases of the apparent mass and cross-axis apparent mass, respectively;  $\Phi_m$  and  $\Phi_{C_m}$ , measured phases of the apparent mass and cross-axis apparent mass, respectively.  $w_1$ ,  $w_2$ , and  $w_3$  are arbitrary weighting factors used to improve the prediction. For initial runs of the prediction process, the values of  $w_1$ ,  $w_2$ , and  $w_3$  were set to 1.0. The weighting factors for the functions (i.e. the moduli and phases of the apparent mass and cross-axis apparent mass) that did not give good prediction were then adjusted by increasing their values until good prediction was achieved. The values of  $w_2$  and  $w_3$  were always higher than the value of  $w_1$  as the numerical values of the phases (in radians) are much smaller than the numerical values of the magnitudes of the apparent mass or the cross-axis apparent mass. The values of the weighting factors differed for different subjects.

At the start of the optimisation procedure, initial guesses were given to each of the 12 parameters in the model and these were then corrected during the optimisation. In most cases the initial guesses led to reasonable predictions that were improved by adjusting the arbitrary weighting factors in the error equation (i.e.  $w_1$ ,  $w_2$ , and  $w_3$ ). In some cases, several initial guesses had to be tried in order to get a good prediction. The dependence of the optimisation on the initial guesses and the weighting factors implies that the solutions obtained may not be unique: different initial guesses and weighting factors lead to different sets of optimised parameters.

## 3. Results

### 3.1. Modelling of median data

Parameters for the model that fitted both the median measured vertical apparent mass and the median measured fore-and-aft cross-axis apparent mass of the 12 subjects were determined. The optimised parameters

Table 1  
Optimised model parameters for the vertical apparent mass and fore-and-aft cross-axis apparent masses of 12 subjects ( $m_1 = 0$ )

Subject	$m_2$ (kg)	$m_3$ (kg)	$J_2$ (kg m <sup>2</sup> )	$k_{1x}$ (N/m)	$k_2$ (N/m)	$k_{3z}$ (N/m)	$c_{1x}$ (N s/m)	$c_2$ (N s/m)	$c_{3z}$ (N s/m)	$e$ (m)	$\alpha$ (rad)
1	26	26	0.29	26,024	142	25,631	2879	2	344	0.07	1.00
2	24	45	0.12	32,887	76	44,264	551	7	406	0.07	0.99
3	21	43	0.18	69,002	90	74,587	1132	1	1135	0.06	1.35
4	16	44	0.14	33,170	41	48,193	694	4	787	0.09	1.33
5	14	35	1.14	41,203	414	40,549	558	14	679	0.28	1.39
6	20	37	0.17	29,561	145	36,458	636	11	296	0.09	0.93
7	20	39	0.08	37,212	67	64,479	660	5	409	0.06	0.96
8	17	36	0.51	44,320	186	35,845	1167	4	545	0.10	1.25
9	17	42	0.13	49,202	49	40,155	758	1	786	0.06	1.27
10	24	35	0.13	19,457	31	21,967	514	7	149	0.07	0.61
11	24	43	0.21	32,545	162	37,923	744	14	445	0.09	0.98
12	23	64	9.41	38,990	12,409	52,602	469	127	936	0.49	1.32
Median	21	41	0.18	35,191	116	40,352	677	6	495	0.08	1.13
Median model	18	41	0.20	33,355	88	43,441	659	7	660	0.11	1.26

are given in the last row of Table 1. The parameters determined by the process allowed the model to fit closely to the measured modulus and phase in both directions.

### 3.2. Modelling of individual data

It was found that the same model could also provide close fits to the responses of each of the 12 individual subjects (Figs. 3–6). In general, a model optimised to the median apparent mass may not be optimum for any individual apparent mass. However, individuals had similar responses and a previous study with solely vertical apparent mass has found that the same form of model can fit both median and individual data with a high accuracy [8].

The parameters of the optimised model for each individual subject are shown in Table 1. The optimised parameters are of a similar order of magnitude for each subject (except for subject 12). For both the median response and the individual responses, the value of  $m_1$  was found to be very small (relative to  $m_2$  and  $m_3$ ) or zero. It was decided to fix the value of  $m_1$  at exactly zero for all subjects.

### 3.3. Parameter sensitivity tests

The effects of changes in the optimised model parameters (masses, stiffness, and damping coefficients) on the resonance frequencies and the magnitudes at resonance in both the vertical apparent mass and the fore-and-aft cross-axis apparent mass were studied. For the predicted median response, each model parameter was allowed to change by  $\pm 40\%$  from the optimised value while the other parameters were fixed at the optimised values. This helps to identify the parts of the model producing the resonance behaviour.

#### 3.3.1. Vertical apparent mass

Changes in the resonance frequency and the magnitude of the apparent mass at resonance of the model response as a result of  $\pm 40\%$  changes in the optimised model parameters are given in Table 2. The table shows that the greatest changes in the resonance frequencies of the apparent mass occurred with changes in  $k_{3z}$  and  $m_3$  (Table 2). The largest changes in the vertical apparent mass at resonance resulted from changes in  $m_3$  and  $c_{3z}$ . It can be concluded that the resonance frequency of the vertical apparent mass is mainly produced by the single degree-of-freedom system represented by  $m_3$ ,  $k_{3z}$  and  $c_{3z}$ .

#### 3.3.2. Fore-and-aft cross-axis apparent mass

Changes of the resonance frequency and the magnitude of the apparent mass at resonance in the predicted median fore-and-aft cross-axis apparent mass with a  $\pm 40\%$  change in the optimised parameters are shown in

Table 2

Resonance frequencies and apparent mass magnitude at resonance calculated after  $\pm 40\%$  change in each model parameter

	Frequency (Hz)		Magnitude (kg)	
	–40%	+40%	–40%	+40%
$m_2$	4.30	4.30	81.27	99.00
$m_3$	5.47	3.91	58.19	121.75
$k_{1,x}$	4.30	4.69	88.22	91.54
$c_{1,x}$	4.30	4.30	91.30	89.36
$k_2$	4.30	4.30	90.01	90.58
$c_2$	4.30	4.30	86.16	92.56
$k_{3,z}$	3.52	5.47	83.11	91.96
$c_{3,z}$	4.69	4.30	111.08	79.89

Initial values were 4.30 Hz and 90.12 kg.

Table 3

Resonance frequencies and fore-and-aft cross-axis apparent mass magnitude at resonance calculated after  $\pm 40\%$  change in each model parameter

	Frequency (Hz)		Magnitude (kg)	
	–40%	+40%	–40%	+40%
$m_2$	4.30	4.30	16.43	19.21
$m_3$	5.86	3.52	7.77	32.77
$k_{1,x}$	3.91	4.69	11.12	26.75
$c_{1,x}$	3.91	4.30	24.87	16.53
$k_2$	4.30	4.30	18.56	19.70
$c_2$	4.30	4.30	24.81	15.63
$k_{3,z}$	3.91	4.69	19.76	16.15
$c_{3,z}$	4.69	3.91	24.54	16.25

Initial values were 4.30 Hz and 19.22 kg.

**Table 3.** The greatest changes in the resonance frequencies of the cross-axis apparent mass occurred with a change in  $m_3$  together with a small change in the resonance frequency due to changes in  $k_{1,x}$ ,  $k_{3,z}$  and  $c_{3,z}$  (Table 3). All parameters had an effect on the magnitude of the cross-axis apparent mass at resonance, with an extent that differed between the parameters: the greatest change came from changing the parameters of the horizontal degree of freedom beneath mass  $m_1$  and the vertical degree of freedom beneath mass  $m_3$ , as well as changing  $c_2$ .

#### 4. Discussion

During the development of the model, not described in this paper, the fore-and-aft degree of freedom beneath mass 1 was found to be necessary to predict both the vertical apparent mass and the fore-and-aft cross-axis apparent mass: an alternative vertical stiffness and damping in place of the horizontal stiffness and damping beneath mass 1 allowed the model to predict the vertical apparent mass but with a poor fit to the fore-and-aft cross-axis apparent mass. Matsumoto and Griffin [15] developed a similar model to that reported in this study but with an extra rotational degree of freedom and with vertical stiffness and damping in place of horizontal stiffness and damping beneath mass 1 (Model 1 in Matsumoto and Griffin [15]). That model was used to predict the vertical apparent mass and vertical and fore-and-aft transmissibilities to different locations on the body and gave a prediction of the apparent mass that was better than the prediction of the



transmissibilities. The prediction of the transmissibilities by the Matsumoto and Griffin model might have been improved with a horizontal degree of freedom beneath the model.

The need for a fore-and-aft degree of freedom is consistent with the human body undergoing fore-and-aft oscillation when exposed to vertical excitation, which may indicate shear deformation of the tissues around the ischial tuberosities. This is consistent with the conclusion of Broman et al. [20] that a vertical, rotational and horizontal sub-system ‘that allows the subject to slide on the seat’ was needed to model experimentally measured vertical transmissibility to the third lumbar vertebra. Kitazaki and Griffin [14] used finite elements to model the apparent mass and the motions of the spine, pelvis, viscera, and the head in the mid-sagittal plane. A third mode of vibration (at 2.81 Hz), a fourth vibration mode (at 5.06 Hz—the principal resonance of the apparent mass) and a fifth vibration mode (at 5.77 Hz) extracted from the model were all reported to include fore-and-aft motion of the pelvis and deformation of the tissue beneath the pelvis. In the present study, the resonance frequencies of the fore-and-aft cross-axis apparent masses of the twelve subjects fell in the range 3.52–5.47 Hz, with some of these frequencies higher and some lower than the resonance frequency of the vertical apparent mass. It may be hypothesised that the three modes reported by Kitazaki and Griffin [14] contributed to the peak of the fore-and-aft cross-axis apparent mass but may not have been separated into three peaks due to the heavy damping of the human body.

Although the model presented in this paper was not intended as a mechanistic model, the masses  $m_2$  and  $m_3$  seem broadly similar to the masses of the pelvis (and the part of the legs supported on the seat) and the upper body without the pelvis, respectively, bearing in mind the simplicity of the model (see data provided by Singley and Haley [21]). The values of the moment of inertia (except for subject 12), and the geometrical parameters of  $m_2$  with respect to a reference located at the ischial tuberosities also seem to be similar to those of the pelvis (see data provided by Singley and Haley [21]), given the simplicity of the model. For example, in the model, the springs and dampers used were assumed to be linear and the parameters were assumed to be independent of time and frequency, although this might not be the case with the properties of the human body (see Ref. [22]). It was also assumed that the centre of gravity of  $m_2$  and the centre of gravity of  $m_3$  have the same fore-and-aft distance from the connection point, although this is not necessarily the case if  $m_2$  and  $m_3$  are the pelvis and the upper body.

The parameter sensitivity test (Section 3.3.1) showed that the resonance in the vertical apparent mass around 4 Hz is produced mainly by vertical motion of  $m_3$ , which might be considered to be vertical motion of the ‘upper body’, including the spine, viscera and head. Hagen et al. [23] measured the transmissibility between a vibrating seat and the spine and between the sacrum and the spine and reported that the principal resonance frequency at 4–5 Hz corresponded to motion of the entire upper body, as in the model presented in this study. Kitazaki and Griffin [14] also reported that ‘a principal resonance of the human body at about 5 Hz consisted of an entire body mode, in which the skeleton moved vertically due to axial and shear deformations of buttocks tissue, in phase with a vertical visceral mode, and a bending mode of the upper thoracic and cervical spine’, although in the present study no axial deformation of the buttocks tissue was needed in the model to reproduce the apparent mass.

Matsumoto and Griffin [15] modelled the vertical apparent mass and the vertical and fore-and-aft transmissibilities to different locations on the spine using models with rotational capabilities and concluded that the resonance frequency at around 5 Hz was ‘attributed to a vibration mode consisting of vertical motion of the pelvis and legs and a pitch motion of the pelvis, both of which cause vertical motion of the upper-body above the pelvis, a bending motion of the spine and vertical motion of the viscera’. A parameter sensitivity test showed that axial deformation of tissue beneath the legs and pelvis (not included in the model presented in this paper) was the main contributor to the resonance frequency of the apparent mass, with some contribution from the vertical motion of the viscera, while the pitch degree of freedom made little contribution to the resonance frequency. A parameter sensitivity test for the model presented in this paper showed that the pitch motion of  $m_2$  made no contribution to the principal resonance frequency of the apparent mass at 5 Hz, while the main contributor to the resonance came from the vertical motion of the upper body.

The median vertical stiffness and damping beneath  $m_3$  (40,352 N/m and 495 N s/m, see Table 1) derived in this study are broadly similar to those obtained by Wei and Griffin [8] for a two-degree-of-freedom model (35,776 and 38,374 N/m for the stiffness and 761 and 458 N s/m for the damping) that moved only vertically

and predicted only the vertical apparent mass. As explained above, the vertical apparent mass of the current model was mainly influenced by the vertical degree of freedom. The similarity between the values of the stiffness and damping in both models is consistent with the vertical apparent mass being primarily influenced by the vertical degree of freedom in both models.

Cho and Yoon [24] modelled the vertical transmissibility to the hip and head and the fore-and-aft transmissibility to the back using a 9 degree-of-freedom model. The model also took into account the dynamic response of the seat and the backrest. The values of fore-and-aft stiffness and damping between the seat and the body (i.e. for the thighs and the ischial tuberosities) obtained from the model were in the range 35,400–57,200 N/m for the stiffness and in the range 280–614 N s/m for the damping, similar to the values obtained in this study for the fore-and-aft degree-of-freedom (35,191 N/m for the stiffness and 677 N s/m for the damping). However, the rotational stiffness and rotational damping found by Cho and Yoon (0 N m for the stiffness and between 1570 and 3583 Nsm for the damping) differ from the present study (116 N m for the stiffness and 6 Nsm for the damping). The difference between the parameters in the two studies may be explained by the different locations for rotational stiffness and damping in the two studies: close to the seat in the present study (as  $m_1 = 0$ , the massless frame can be removed and the connection point can be considered to be on the seat) and between the pelvis and the upper body in the study by Cho and Yoon. The difference between the values may also be explained by the different seating conditions in the studies. In the present study there was no backrest while Cho and Yoon had an inclined backrest. Resting the upper body on an inclined backrest may allow the body to maintain posture without muscular action, explaining the 0 N m rotational stiffness obtained by Cho and Yoon. A rotational stiffness was needed in the present study without a backrest to keep the body stable. Matsumoto and Griffin [15] reported a similar value for the rotational damping (6.72 N s m) to that found in this study (6 N s m) but they found a greater rotational stiffness (477 N m) than in this study (116 N m).

The parameter sensitivity study showed that the resonance frequency of both the vertical apparent mass and the fore-and-aft cross-axis apparent mass were affected when changing the parameters of the vertical degree of freedom (i.e.  $m_3$ ,  $k_{3z}$  and  $c_{3z}$ ). This is consistent with the experimental results where the resonance frequency of the vertical apparent mass and the fore-and-aft cross-axis apparent mass were found to be correlated [1]. However, Nawayseh and Griffin [3] reported that the correlation between the resonance frequency of the vertical apparent mass and the resonance frequency of the fore-and-aft cross-axis apparent mass depended on leg posture: they found no correlation between the two resonance frequencies with stretched lower legs as opposed to a posture with vertical lower legs as used by Nawayseh and Griffin [1]. This suggests that the mechanisms contributing to the resonance frequencies change with posture such that when common mechanisms contribute to both the vertical resonance and the fore-and-aft resonance a correlation can be found, but when there is no common mechanisms there is no correlation. The vertical apparent mass reported in the two studies (i.e. Refs. [1,3]) are similar despite the different leg postures. However, the fore-and-aft cross-axis apparent masses were very different in the two studies. The cross-axis apparent mass has also been reported to depend on muscle tension [25] and the presence of a backrest [2]. The cross-axis transfer functions and their dependence on the vibration magnitude differed between tensed and relaxed upper-body muscles [25]. The use of a vertical backrest also modified the fore-and-aft cross-axis apparent mass on the seat surface [2]. Consequently, the model developed in this study may not fit the responses of subjects sitting in all postures: the parameters of the model, and possibly the vibration modes in the model, may change with posture and muscle tension.

The human body has shown a nonlinear response in both the vertical apparent mass and the fore-and-aft cross-axis apparent mass (e.g. Refs. [1–3]). The data used to optimise the parameters of the model presented in this paper were obtained at a vibration excitation of  $1.25 \text{ m s}^{-2}$  rms. Some of the parameters in the model will differ when using a different excitation magnitude.

The human body absorbs power when exposed to vibration. The absorbed power can be calculated from the force and velocity measured in the same direction. Previous studies measured the total absorbed power by the body during vertical excitation (e.g. Refs. [26,27]). The model developed in this paper suggests that fore-and-aft motion of the body on the seat during vertical excitation will be associated with the absorption of power in the fore-and-aft direction. Further work may quantify the percentage of the power absorbed in the fore-and-aft direction during vertical excitation.

## 5. Conclusions

A lumped parameter model with a vertical, a horizontal, and a rotational degree-of-freedom has been developed to fit the moduli and phases of the vertical apparent masses and fore-and-aft cross-axis apparent masses of persons sitting on a rigid seat with no backrest during vertical excitation. By an analogy to the human body, the resonance frequency of the vertical apparent mass was attributed to vertical motion of the upper body. The resonance frequency of the fore-and-aft cross-axis apparent mass was attributed to fore-and-aft motion of the body on the seat as well as the vertical motion of the body.

The stiffnesses and damping of the model are in good agreement with the stiffness and damping obtained in relevant previous studies using both more simple and more complex models than presented here.

## References

- [1] N. Nawayseh, M.J. Griffin, Non-linear dual-axis biodynamic response to vertical whole-body vibration, *Journal of Sound and Vibration* 268 (2003) 503–523.
- [2] N. Nawayseh, M.J. Griffin, Tri-axial forces at the seat and backrest during whole-body vertical vibration, *Journal of Sound and Vibration* 277 (2004) 309–326.
- [3] N. Nawayseh, M.J. Griffin, Effect of seat surface angle on forces at the seat surface during whole-body vertical vibration, *Journal of Sound and Vibration* 284 (2005) 613–634.
- [4] Y. Matsumoto, M.J. Griffin, Movement of the upper-body of seated subjects exposed to vertical whole-body vibration at the principal resonance frequency, *Journal of Sound and Vibration* 215 (1998) 743–762.
- [5] M. Fritz, Description of the relation between the forces acting in the lumbar spine and whole-body vibrations by means of transfer functions, *Clinical Biomechanics* 15 (2000) 234–240.
- [6] C.W. Suggs, C.F. Abrams, L.F. Stikeleather, Application of a damped spring-mass human vibration simulator in vibration testing of vehicle seats, *Ergonomics* 12 (1969) 79–90.
- [7] T.E. Fairley, M.J. Griffin, The apparent mass of the seated human body: vertical vibration, *Journal of Biomechanics* 22 (1989) 81–94.
- [8] L. Wei, M.J. Griffin, The prediction of seat transmissibility from measures of seat impedance, *Journal of Sound and Vibration* 214 (1998) 121–137.
- [9] International Organization for Standardization, International Standard ISO 5982, Mechanical vibration and shock—range of idealised values to characterise seated body biodynamic responses under vertical vibration, 2001.
- [10] P.-E. Boileau, S. Rakheja, Whole-body vertical biodynamic response characteristics of the seated vehicle driver: measurement and model development, *International Journal of Industrial Ergonomics* 22 (1998) 449–472.
- [11] Y. Matsumoto, M.J. Griffin, Mathematical models for the apparent masses of standing subjects exposed to vertical whole-body vibration, *Journal of Sound and Vibration* 260 (2003) 431–451.
- [12] N.J. Mansfield, R. Lundstrom, Models of the apparent mass of the seated human body exposed to horizontal whole body vibration, *Aviation, Space and Environmental Medicine* 70 (1999) 1166–1172.
- [13] G.J. Stein, P. Mucka, R. Chmurny, Preliminary results on an  $x$ -direction apparent mass model of human body sitting in a cushioned, suspended seat, *Journal of Sound and Vibration* 298 (2006) 810–823.
- [14] S. Kitazaki, M.J. Griffin, A modal analysis of whole-body vertical vibration, using a finite element model of the human body, *Journal of Sound and Vibration* 200 (1997) 83–103.
- [15] Y. Matsumoto, M.J. Griffin, Modelling the dynamic mechanisms associated with the principal resonance of the seated human body, *Clinical Biomechanics* 16 (2001) S31–S44.
- [16] N. Nawayseh, Cross-axis Movements of the Seated Human Body in Response to Whole-body Vertical and Fore-and-aft Vibration, PhD Thesis, University of Southampton, 2004.
- [17] B. Hinz, R. Blüthner, G. Menzel, S. Rützel, H. Seidel, H.P. Wölfel, Apparent mass of seated men—determination with single- and multi-axis excitations at different magnitudes, *Journal of Sound and Vibration* 298 (2006) 788–809.
- [18] N.J. Mansfield, S. Maeda, The apparent mass of the seated human exposed to single-axis and multi-axis whole-body vibration, *Journal of Biomechanics* 40 (2007) 2543–2551.
- [19] Y. Matsumoto, K. Ohdo, T. Saito, Dynamic and subjective responses of seated subjects exposed to simultaneous vertical and fore-and-aft whole-body vibration: the effect of the phase between the two single-axis components, *Journal of Sound and Vibration* 298 (2006) 773–787.
- [20] H. Broman, M. Pope, T. Hansson, A mathematical model of the impact response of the seated subject, *Medical Engineering and Physics* 18 (1996) 410–419.
- [21] G.T. Singley, J.L. Haley, The use of mathematical modeling in crashworthy helicopter seating system, *AGARD Conference Proceedings*, No. 253, A22-1-21, Paris, France, 1979.
- [22] R. Muksian, C.D. Nash, On frequency-dependent damping coefficients in lumped-parameter models of human beings, *Journal of Biomechanics* 9 (1976) 339–342.
- [23] F.W. Hagena, C.J. Wirth, J. Piehler, W. Plitz, W.G.O. Hofmann, T. Zwingers, In vivo experiments on the response of the human spine to sinusoidal G<sub>z</sub>-vibration, *AGARD Conference Proceeding*, No.378, Pozzuoli, Italy, 1985.

- [24] Y. Cho, Y.S. Yoon, Biomechanical model of human on seat with backrest for evaluating ride quality, *International Journal of Industrial Ergonomics* 27 (2001) 331–345.
- [25] N.J. Mansfield, P. Holmlund, R. Lundstrom, P. Lenzuni, P. Nataletti, Effect of vibration magnitude, vibration spectrum, and muscle tension on apparent mass and cross-axis transfer functions during whole-body vibration exposure, *Journal of Biomechanics* 39 (2006) 3062–3070.
- [26] N.J. Mansfield, M.J. Griffin, Effect of magnitude of vertical whole-body vibration on absorbed power for the seated human body, *Journal of Sound and Vibration* 215 (1998) 813–825.
- [27] N. Nawayseh, Absorbed power at the seat, backrest and feet of subjects exposed to whole-body vertical vibration. *40th United Kingdom Conference on Human Responses to Vibration*, Liverpool, England, 2005.